In the Name of Allah, The Most beneficiary,
The Most Gracious, The Most Merciful

Computational Study of Falkner-Skan Problem for a Static and Moving Wedge

By

Shafiq Ahmad.

Department of Mathematics
Quaid-i-Azam University
Islamabad, Pakistan
2017

Computational Study of Falkner-Skan Problem for a Static and Moving Wedge.

By

Shafiq Ahmad

Supervised By

Dr. Sohail Nadeem.

Department of Mathematics
Quaid-i-Azam University
Islamabad, Pakistan
2017

Computational Study of Falkner-Skan Problem for a Static and Moving Wedge.

By

Shafiq Ahmad

A DISSERTATION SUBMITTED IN THE PARTIAL FULFILLMENT OF THE REQUIREMENT FOR THE DEGREE OF

MASTER OF PHILOSOPHY

IN

MATHEMATICS

Supervised By

Dr. Sohail Nadeem.

Department of Mathematics
Quaid-i-Azam University
Islamabad, Pakistan
2017

Acknowledgments

In the name of ALLAh, the most Beneficent, who enabled me to complete my dissertation. I offer my humble gratitude to Holy Prophet MUHAMMAD (peace Be Upon Him), who is forever a touch of guidance and knowledge for humanity as a whole.

I feel highly privileged to express my heartfelt gratitude to my supervisor, Prof. Dr. Sohail Nadeem for his skilful guidance, helpful suggestions and inspiring attitude during the research. His kindness and generous response to my difficulties during the research work to complete the dissertation in time will never forgotten.

I am also thankful to all the teaching staff of our department. Their inspiration and suggestions helped me to complete my research work.

I would like to extend my sincere gratitude to my friends, Noor Muhammad, Arif Ullah, Latif, Naeem Ullah and Abdul Hafeez who have supported me and given me confidence to complete this task.

At the end, my appreciation is also expressed to my parents, brothers, wife and other family members for their constant support, love, guidance and encouragement throughout my career.

Shafiq Ahmad

July 2017.

Preface

The study of the heat transport phenomena in fluid flows got extensive attention due to its wide applications in industries and nano-technology. Nanofluids are suspensions of nanometer-sized particle with base fluids. The base fluids are usually taken as water, kerosene oil, or some other solvent. Thermal conductivity is larger in a nanofluid as compared to base fluid [1,2]. The nano-sized particles are made up of carbide, metal, metal oxide, nitride and some other nano-scale fluid droplets [3]. The shape and structure of the nanoparticles can be rod-like, spherical or tubular like and dispersed individually. Choi [4] initiated the new class of nano fluids. Nano fluids usually flow smoothly inside the micro channels. These fluids behave like normal fluids due to small size of the nanoparticles [5]. Haq et al. [6] exposed the impact of heat transfer analysis in a squeezed flow over a sensor surface in the presence of magneto hydrodynamic. Lin et al. [7] introduced the influence of heat transfer analysis in a magneto hydrodynamic pseudo-plastic nanofluid flow over a stretching surface in the presence of internal heat generation. Nadeem and Muhammad [8] scrutinized the impact of Cattaneo Christov heat and mass flux in a nanofluid imbedded in a porous medium. Nadeem and Lee [9] considered the exponentially stretching surface to discuss the boundary layer flow of nanofluid.

The phenomena of induced magnetic field are applicable in several physical situations. The scientist and mathematician worked the field of induced magnetic field. Some applications of the phenomena of induced magnetic field may be seen in [10, 11]. Kumari et al. [12] examined the heat transfer and MHD flow over a stretching surface by considering the impact of the induced magnetic field, Takhar et al. [13] contemplated the unsteady free convection flow at the stagnation point under the effect of a magnetic field. Ali et al. [14] interrogated the heat transfer and MHD stagnation point flows towards a stretching sheet by contemplate the impact of the induced

magnetic field. Nadeem and Akram [15] investigated the peristaltic flow of a couple stress fluid in an asymmetric channel by taking the influence of induced magnetic field. Mekheimer [16] explored the impact of induced magnetic field on peristaltic flow of a couple stress fluid. The exact solution of temperature appropriation on the steady flow over a stretching sheet has been highlighted by Dutta [17] for MHD flow of a viscous and electrically conducting fluid within the sight of a constant magnetic field. This problem has been likewise considered by Andersson [18], and Pop and Na [19]. Devi and Thiyagarajan [20] explored the nonlinear hydromagnetic steady flow and heat transfer past a stretching sheet with variable temperature. Ali et al. [22, 23] scrutinized the impact of an induced magnetic field on boundary layer flow over a stretching surface.

The liquid flow due to a moving wedge is an important phenomenon. In such phenomenon, the fluid and plate velocities are proportional to each other, this is an applicable in sundry engineering processes. For instance, the thermal processing of sheet like substance is an essential operation in the preparation of paper, wire drawing, linoleum, drawing of plastic films, polymeric sheets, fine fibber matts and metal spinning. In all the above processes and application, the moment of sheet is parallel to its own plane. The sheet may reduce the movements of particles in the neighboring fluid or the fluid may have a forced convection motion which is parallel to that of the sheet. The flow of fluids over a moving wedge is explored by Abraham and sparrow [24, 25]. Sakiadis [26] proposed the fluid flows over a moving wedge with a constant speed in a quiescent fluid medium. Yacob et al. [27] investigated Falkner-Skan problem for a moving or static wedge in a nanofluid. Asaithambi [28] utilized finite difference method to get solutions for $-0.19884 \leq \beta \leq 2$. Zaturska and Banks [29] examined diagnostically the case $\beta > 1$. Yang and Chang [30] introduced analytical answer for $\beta = -1$ for a stable plate. Recently, Fang and Zhang [31] displayed an

investigative solution for a moving and penetrable wall when β = -1. The present analysis is the extension of the work of Yacob et al. [27]. These analyses characterized the impacts of heat transfer analysis in Falkner-Skan problem via static or moving wedge in the presence of induced magnetic field in a nanofluid with $0 \leq \beta \leq 1$. Keep in mind that β=0 corresponds to horizontal plate, on the other hand β=1 corresponds to a vertical plate. The boundary value problem is solved via shooting technique. The characteristic of solid volume friction on the heat transfer rate are analyzed and discussed. It is observed that the thermal conductivity arises for nanofluid as compared to regular fluid.

Keeping the above highlights in mind, the dissertation is arranged as follows, in chapter 1, we have defined some basic definitions of fluid mechanics.

Chapter 2, is devoted to analyzed the heat and mass transfer of a Falkner-Skan problem for a moving and static wedge in nanofluids. The effect of emerging parameters on the axial velocity and temperature field is highlighted and scrutinized graphically.

In chapter 3, we have examined the Falkner-Skan problem Falkner-Skan problem in the flow of a nanofluids in presence of induced magnetic field. The transformed equations are solved numerically by using Rung-Kutta technique. Finally, the impact of the emerging flow parameters is plotted and discussed through several graphs.

Contents

Chapter 1

Basic definitions

1.1 Preliminaries

In this chapter, we illustrate some fundamental definitions and governing laws for better understanding of fluid problem.

1.2 Basic definitions

1.2.1 Fluid

A substance which deforms constantly under the effect of shear stress is termed as fluid.

1.2.2 Flow

The persistently change in the shape of material without any limit under the influence of applied forces is called flow.

1.2.3 Fluid mechanics

Fluid mechanics is a field of mechanics that deals the characteristic of fluid and forces applied on it. Furthermore, it has two sub branches i.e. fluid dynamic and fluid statics.

The characteristic of moving fluid is studied in fluid dynamics. While fluid statics deals with the properties of stationary fluid.

1.2.4 Stress

Stress is a force which acts on the unit surface area in a deformable body. The below equation is utilized to compute the stress.

$$Stress = \frac{force}{area} = \frac{F}{A} \tag{1.1}$$

The SI unit of stress is $kg / m.s^2$ or Pa (Pascal) and dimension $\left[\frac{M}{LT^2}\right]$. Further two components of stress are,

(i) Shear stress

Shear stress is expressed as the force acting parallel to surface unit area.

(ii) Normal stress

Normal stress is the force which are acting perpendicular to surface unit area.

1.2.5 Strain

The non-dimensional quantity which is used to measure the deformation of a material brought on by the applied forces is named as strain.

1.3 Some physical properties of fluids

1.3.1 Density

Density of fluid is a considerable property which demonstrates a connection between mass of fluid and tiny volume of fluid. The symbol frequently utilized for density is ρ (the lower case Greek letter rho).

Mathematically define as

$$\rho = \lim_{\delta v \to 0} \frac{\delta m}{\delta v}. \tag{1.2}$$

The SI unit of density is kg / m^3 and dimension is $[\frac{M}{L^3}]$.

1.3.2 Viscosity

Viscosity is an intrinsic fluid property which measure as the fluid resistance against its deformation. Viscosity is proportional to shear stress times to inverse of rate of shear strain. Mathematically, it can be written as i.e.

$$\text{viscosity} = \frac{1}{\text{rate of shear strain}} \times \text{shear stress.}$$

Where μ identify the dynamic viscosity, the SI unit and dimension of viscosity is $kg/m.s$ and $\left[\frac{M}{LT}\right]$ respectively.

1.3.3 Kinematic viscosity (υ)

The kinematic viscosity (momentum diffusivity) is proportional to the quotient of μ dynamic viscosity to ρ density of the fluid. The mathematical expression is

$$\upsilon = \frac{\mu}{\rho}. \tag{1.3}$$

In which υ denote the kinematic viscosity. In mechanics, the SI unit of υ (kinematic viscosity) is m^2/s and dimension is $\left[\frac{L^2}{T}\right]$.

1.3.4 Thermal conductivity

The heat conducting capacity of a substance is known as thermal conductivity. It is symbolized by *k* and evaluated from Fourier law of heat conduction that is

$$\vec{\mathbf{q}} = -k\nabla\mathbf{T} \tag{1.4}$$

Here $\vec{\mathbf{q}}$ indicate local heat flux density and $\mathbf{T}$ reveal the temperature. Its SI unit is W/mK and $[\frac{ML}{T^3\Theta}]$ is its dimension. It experimentally demonstrates that thermal conductivity differs linearly

when temperature rises.

1.3.5 Thermal diffusivity

We characterize the thermal diffusivity of a material as “the ratio between the thermal conductivity of a material and the product of specific heat and density at consistent pressure”.

Mathematically, the thermal diffusivity communicated as

$$\alpha = \frac{k}{\rho c_p}. \tag{1.5}$$

The dimension of thermal diffusivity is $[L^2 / T]$ and its SI unit is m^2 / s.

1.4 Types of flows

1.4.1 Laminar flow

Laminar flow is the sort of flow in which every fluid particle has particular paths and do not cross the paths of each other. We observe the smoke rising from a cigarette. For the first few centimeters the flow is certainly laminar and then becomes turbulent.

1.4.2 Turbulent flow

It is the sort of flow where particles of the fluid have no particular paths furthermore these paths of particular particles cross each other.

1.4.3 Incompressible flow

The fluid having constant density in the entire flow field is called incompressible flow.

Incompressible flow mathematically expressed as

$$\rho \neq \rho(x, y, z, t) \tag{1.6}$$

i.e. ρ is constant.

Or

$$\nabla.\mathbf{V} = 0, \tag{1.7}$$

also, known as continuity equation for incompressible flow.

1.4.4 Compressible flow

Compressible flows are those in which the density of fluid does not remain constant throughout the flow channel.

Mathematically it can be composed as

$$\rho = \rho(x, y, z, t). \tag{1.8}$$

1.4.5 Steady flow

A fluid flows whose characteristics don't change with the passage of time is known as steady flow.

Mathematically is defined as

$$\frac{\partial \eta}{\partial t} = 0. \tag{1.9}$$

Here η is the fluid property.

1.4.6 Unsteady flow

The properties of the flow that change at every point with time or it is time dependent.

Mathematical form of unsteady flow is

$$\frac{\partial \eta}{\partial t} \neq 0. \tag{1.10}$$

1.5 Nanofluid

Nanofluid are another group of nanotechnologies based fluids made by scattering nanometer-sized

particle with normal length scale on the order of (1-100nm) in customary heat transfer fluids. These particles can be found in the metal such as (Cu, Al), oxides (Al_2O_3) Carbides (SiC) or nonmetal (Nanotubes, Carbon, Graphite).

1.5.1 Density of nanofluids

The density of nanofluid is expressed as

$$\rho_{nf} = (1-\phi)\rho_f + \phi\rho_s. \tag{1.11}$$

Here ϕ are the solid volume friction, ρ_s and ρ_f respectively the density of solid particle and base fluid.

1.5.2 Viscosity of nanofluids

Brinkman [35] presented a viscosity model of nanofluid as a function of volume friction

$$\mu_{nf} = \frac{\mu_f}{(1-\phi)^{2.5}}. \tag{1.12}$$

In above equation μ_{nf} suggest the density of nanofluids and μ_f mean the density of base fluid.

1.5.3 Nanofluids heat capacity

The heat capacity of nanofluids is denoted by $(\rho C_p)_{nf}$ is expressed as

$$(\rho C_p)_{nf} = \phi(\rho C_p)_s + (1-\phi)(\rho C_p)_f. \tag{1.13}$$

Here $(\rho C_p)_s$ and $(\rho C_p)_f$ demonstrate the heat capacity of solid particle and base fluid respectively.

1.6 Governing law

1.6.1 Law of conservation of mass

This law describes that in a closed system, the mass of the system cannot change over time

means it can neither be created nor be destroyed although it may change its shape. In vectorially form it is defined as

$$\frac{\partial \rho}{\partial t} + \nabla.(\rho \mathbf{V}) = 0, \tag{1.14}$$

Here ρ characterize the density, ∇ identify the differential operator and $\mathbf{V}$ exemplify the velocity field. For incompressible fluid, the above equation become as

$$\nabla.\mathbf{V} = 0. \tag{1.15}$$

1.6.2 Law of conservation of momentum

Law of conservation of momentum is another form of Newton's second law. It is defined that for an isolated system combine effect of all forces is proportional to time rate of change of momentum.

Mathematical form is

$$\rho \frac{d\mathbf{V}}{dt} = \operatorname{div} \boldsymbol{\tau} + \rho \mathbf{B}. \tag{1.16}$$

Here $\mathbf{B}$ is the body forces, $\boldsymbol{\tau}$ demonstrate the Cauchy stress tensor and d/dt imply the material derivative, expressed as

$$\frac{d}{dt} = \frac{\partial}{\partial t} + (\nabla.\mathbf{V}), \tag{1.17}$$

$$\boldsymbol{\tau} = -p\mathbf{I} + \mu \mathbf{A}_1, \tag{1.18}$$

$\mathbf{A}_1$ mark the Rivlin-Erickson tensor, mathematically written as

$$\mathbf{A}_1 = (\operatorname{grad} \mathbf{V})^{\mathbf{T}} + (\operatorname{grad} \mathbf{V}) \tag{1.19}$$

For two-dimension velocity field, the matrix form of Cauchy stress tensor is expressed as

$$\boldsymbol{\tau} = \begin{pmatrix} \sigma_{xx} & \tau_{xy} \\ \tau_{yx} & \sigma_{yy} \end{pmatrix}. \tag{1.20}$$

Here τ_{xy} and τ_{yx} are shear stresses and σ_{xx}, σ_{yy} are the normal stresses.

1.6.3 Law of conservation of energy

For an isolated system, the law of conservation of energy says that the total energy remains constant i.e. neither created nor destroyed but it transforms from one form to another.

Its mathematical form is

$$\left(\rho C_p\right)_f \left(\frac{\partial}{\partial t} + \mathbf{V}.\boldsymbol{\nabla}\right) T = k\boldsymbol{\nabla}^2 T + \boldsymbol{\tau}.\mathbf{L}. \tag{1.21}$$

Here k shows the thermal conductivity, $\boldsymbol{\tau}.\mathbf{L}$ intimate the representation of viscous dissipation and C_p represent the specific heat.

1.7 Some useful dimensionless numbers

1.7.1 Prandtl number (Pr)

The ratio between kinematic viscosity and thermal conductivity/diffusivity is measured as Prandtl number. Mathematically, it is expressed as

$$\mathrm{Pr} = \frac{\upsilon}{\alpha}. \tag{1.22}$$

1.7.2 Reynolds number

Dimensionless quantity that describes “the ratio of inertial forces to viscous forces is known as Reynolds number”. Physically it determines the flow behavior, weather flow is laminar or turbulent. For turbulent flow Re is large while it is small for laminar flow.

Mathematical form is

$$\mathrm{Re} = \frac{UL}{\upsilon}, \tag{1.23}$$

In above equation L imply the length, U identify the fluid velocity and υ intimate the kinematic viscosity.

1.7.3 Nusselt number

Nusselt number is a unit less quantity and gives ratio of convective heat transfer to conductive heat transfer over the boundary layer and can be communicated as

$$Nu = \frac{hL}{k}. \tag{1.24}$$

Here L is the reference length, h shows convective heat transfer and k designate the thermal conductivity of the fluid.

1.7.4 Skin friction

The friction which occurs between the solid surface and moving fluid to slow down the fluid motion is termed as Skin friction.

Mathematically, drag force is defined as

$$C_f = \frac{\tau_{yx}}{\rho U^2 / 2}. \tag{1.25}$$

Here τ_{yx} is used to denote shear stress, ρ is the density and U is ambient velocity.

1.8 Boundary layer

Ludwing Prandtl gives thought of boundary layer. Boundary layer is really the region closed to the surface where upon fluid flows, here the influence of viscosity is significant and these effects vanish far from the solid boundary as the velocity is called free-stream velocity. By utilizing this idea Navier Stokes equations are simpler to solve.

1.9 Falkner-Skan flow and transformation

In 1930 Falkner and Skan has found the class of self-similar boundary layer flows within the sight of a pressure gradient. This flow is an external flow with a pressure gradient. The flows over wedge shaped bodies are used to portray the Falkner-Skan flow. We consider the boundary layer equations,

$$\frac{\partial u}{\partial x}+\frac{\partial v}{\partial y}=0, \tag{1.26}$$

$$u\frac{\partial u}{\partial x}+v\frac{\partial u}{\partial y}=\frac{\mu}{\rho}\frac{\partial^2 u}{\partial y^2}-\frac{1}{p}\frac{\partial p}{\partial x}. \tag{1.27}$$

In above equation

$$-\frac{1}{p}\frac{\partial p}{\partial x}=U\frac{\partial U}{\partial x}. \tag{1.28}$$

Here U symbolizes the free stream velocity and proportional to x^m

$$U\propto x^m \qquad \text{or} \qquad U=ax^m \tag{1.29}$$

Where m and a are constants. The similarity variables for the Falkner-Skan flow is defined as

$$\eta=\sqrt{\frac{(m+1)ax^{m-1}}{2\nu}}y, \qquad \psi=\sqrt{\frac{2\nu ax^{m+1}}{m+1}}f(\eta) \tag{1.30}$$

Using the above equations in Eq. (1.23) to (1.25), we get

$$f'''+ff''-\beta(f'^2-1)=0, \tag{1.31}$$

With boundary equations

$$f'(0)=0,\ \ f(0)=0,\quad f'(\infty)=1. \tag{1.32}$$

Here

$$\beta = \frac{2m}{m+1} \tag{1.33}$$

The Eq. (1.31) termed as Falkner-Skan equation. The flat plate occur when *m=0* (or β *=0*) and for this value Eq. (1.31) reduces to Blasius equation (named after Richard Heinrich Blasius) and for *m*=1 (or β =1) it reduces to 2D stagnation point flow and β = -0.1988 for the separated flow. The parameter β indicates the behavior of pressure gradient. The pressure gradient is favorable or negative for positive value of β while adverse or positive for negative value of β**.** Further, for separated flow the value of β indicates the point where the pressure gradient is zero.

.

Chapter 2

Falkner-Skan problem for a moving and static wedge in nanofluids

2.1 Introduction

In this chapter, two-dimensional steady flow in presence of moving or static wedge submerged in nanofluids is examined numerically. The governing partial differential equation of the system are transformed into set of nonlinear ordinary differential equations with the help of appropriate similarity transformation. The transformed ordinary differentials equations are solved numerically by using the shooting technique. Three distinct sorts of nanoparticles, in particular titania TiO_2, copper Cu and alumina Al_2O_3 with water base fluid are examined. The parameters which used in the problem are ϕ (solid volume friction), β (Hartee pressure gradient), λ (the moving wedge parameter) and Pr (Prandtl number). The influence of these parameters on heat transfer and flow of fluid are examined in tables and figures. It is depicted that Cu-water has the most noteworthy the heat transfer rate and wall shear stress at the surface contrasted and the other. The numerical values of local Nusselt number and wall shear stresses have been computed and scrutinize. The work in this chapter is a review of the research paper [27].

2.2 Mathematical formulation

Two-dimension Falkner-Skan flow passing through a static or moving wedge containing different

types of nanoparticles such as: Al_2O_3, TiO_2, and Cu. Water is used as a base fluid are incorporated. The (x, y) coordinates are utilized as a part of which x-axis is parallel to the plate and y-axis perpendicular to it, and (u, v) are the respective velocity components.

The equation of continuity and equation of motion for incompressible flow are stated as

$$\nabla.\mathbf{V} = 0, \tag{2.1}$$

$$\rho \frac{d\mathbf{V}}{dt} = \operatorname{div} \boldsymbol{\tau} + \rho \mathbf{b}, \tag{2.2}$$

Where ∇ indicates differential operator, $\mathbf{V}$ symbolize the fluid velocity, ρ signify the fluid density, d/dt symbolized the material time derivative, $\mathbf{b}$ symbolize the body force per unit volume and $\boldsymbol{\tau}$ expresses Cauchy stress tensor. In the absence of the body forces Eq. (2.2) becomes

$$\rho \frac{d\mathbf{V}}{dt} = \operatorname{div} \boldsymbol{\tau}. \tag{2.3}$$

For the present flow ∇, $\mathbf{V}$ and $\boldsymbol{\tau}$ are mathematically expressed as

$$\nabla = \left(\frac{\partial}{\partial x}, \frac{\partial}{\partial y}\right), \tag{2.4}$$

$$\frac{d}{dt} = \frac{\partial}{\partial t} + \mathbf{V}.\nabla, \tag{2.5}$$

$$\mathbf{V} = \left[u(x,y),\ v(x,y),\ 0\right], \tag{2.6}$$

$$\boldsymbol{\tau} = -p\mathbf{I} + \boldsymbol{\mu}\mathbf{A}_1. \tag{2.7}$$

In above expression, $p\mathbf{I}$ indicate the intermediate part of the stress, $\mathbf{A_1}$ designates the first Rivlin-Ericksen tensor (kinematic tensor) and $\boldsymbol{\mu}$ represent the dynamic viscosity is written as

$$\mathbf{A}_1 = \nabla.\mathbf{V} + (\nabla.\mathbf{V})^{\mathrm{T}}, \tag{2.8}$$

here $\nabla.\mathbf{V}$ is expressed as

$$\nabla.\mathbf{V} = \begin{pmatrix} \partial u/\partial x & \partial u/\partial y \\ \partial v/\partial x & \partial v/\partial y \end{pmatrix}. \tag{2.9}$$

After substituting Eq. (2.9) in Eq. (2.8) we acquired $\mathbf{A_1}$ as

$$\mathbf{A_1} = \begin{pmatrix} 2\,\partial u/\partial x & \partial u/\partial y + \partial v/\partial x \\ \partial u/\partial y + \partial v/\partial x & 2\,\partial v/\partial y \end{pmatrix}. \tag{2.10}$$

Putting Eqs. (2.4) to (2.10) in Eqs. (2.1) and (2.3) the continuity and the momentum equations in *x* and *y* component

$$\frac{\partial u}{\partial x} + \frac{\partial v}{\partial y} = 0, \tag{2.11}$$

$$u\frac{\partial u}{\partial x} + v\frac{\partial u}{\partial y} = \upsilon_{nf}\left(\frac{\partial^2 u}{\partial y^2} + 2\frac{\partial^2 u}{\partial x^2}\right) - \frac{1}{\rho}\frac{\partial P}{\partial x}. \tag{2.12}$$

$$u\frac{\partial v}{\partial x} + v\frac{\partial v}{\partial y} = \upsilon_{nf}\left(2\frac{\partial^2 v}{\partial y^2} + \frac{\partial^2 v}{\partial x^2}\right) - \frac{1}{\rho}\frac{\partial P}{\partial y}. \tag{2.13}$$

Now we utilize the boundary layer estimation with the assumption as

$$\begin{aligned} &O(x) = O(1), \quad O(y) = O(\delta), \quad O(u) = O(1), \quad O(v) = O(\delta), \\ &O(\upsilon) = O(\delta^2). \end{aligned} \tag{2.14}$$

After applying the boundary layer approximation given in above equation, Eqs. (2.11) to (2.13) reduced to

$$\frac{\partial u}{\partial x} + \frac{\partial v}{\partial y} = 0, \tag{2.15}$$

$$u\frac{\partial u}{\partial x} + v\frac{\partial u}{\partial y} = \upsilon_{nf}\frac{\partial^2 u}{\partial y^2} - \frac{1}{\rho}\frac{\partial P}{\partial x}. \tag{2.16}$$

The corresponding boundary conditions for the two types of wedge are stated as

i) Static wedge

$$v\big|_{y=0} = 0, \qquad u\big|_{y=0} = 0,$$
$$u\big|_{y\to\infty} \to u_e(x) = U_\infty x^m. \tag{2.17}$$

ii) Moving wedge

$$v\big|_{y=0} = 0, \quad u\big|_{y=0} = u_w(x) = U_w x^m$$
$$u\big|_{y\to\infty} \to u_e(x) = U_\infty x^m. \tag{2.18}$$

Under the boundary layer approach and using the boundary condition at infinity, the pressure gradient term can be computed as

$$-\frac{1}{\rho}\frac{\partial P}{\partial x} = u_e(x)\frac{\partial u_e(x)}{\partial x}, \tag{2.19}$$

Making use of above equation, Eq. (2.16) take the form

$$u\frac{\partial u}{\partial x} + v\frac{\partial u}{\partial y} = u_e(x)\frac{\partial u_e(x)}{\partial x} + \upsilon_{nf}\frac{\partial^2 u}{\partial y^2}. \tag{2.20}$$

Where (u, v) are the respective velocity component along the (x, y) axes. Here $u_w(x) = U_w x^m$ and $u_e(x) = U_\infty x^m$ respectively the velocity of the moving wedge and ambient flow, where U_w, m and U_∞ are constants with $0 \le m \le 1$, the density and viscosity of nanofluid are identified by ρ_{nf} and μ_{nf} respectively, which are given below

$$\mu_{nf} = \frac{\mu_f}{(1-\phi)^{25/10}}, \quad \rho_{nf} = \phi\rho_s + (1-\phi)\rho_f. \tag{2.21}$$

In above equations μ_f explain the viscosity of base fluid, ϕ justify the solid volume friction, ρ_f denote the density of the base fluid and ρ_s assign the density of the solid particle. The thermophysical properties of the nanofluids and base fluid (water) are given in table 2.1.

Thermo-Physical properties	Cu	Al_2O_3	TiO_2	Fluid phase (water)
K(W/mK)	400.0	40.0	8.9538	0.6130
C_p(J/kg K)	385.0	765.0	686.2	4179
ρ (kg/m^3)	8933.0	3970.0	4250	997.10
$\propto \times 10^{-7}$(m^2/s)	1163.10	131.70	30.70	1.470

Table 2.1 The thermophysical properties of base fluid and solid particles are shown.

The energy equation for the present case is

$$\rho c_p \frac{dT}{dt} = \boldsymbol{\tau}.\mathbf{L} - \operatorname{div}\mathbf{q}, \tag{2.22}$$

$$\mathbf{q} = -k_1 \operatorname{grad} T, \tag{2.23}$$

here c_p indicate the specific heat, ρ characterize the density of fluid, $\boldsymbol{\tau}$ specify the Cauchy stress tensor, $\mathbf{L}$ denote the velocity gradient, T demonstrate the temperature, $\mathbf{q}$ communicate the heat flux and k_1 declare the thermal conductivity of fluid. Therefore using Eq. (2.23) in Eq. (2.22) and in the absence of viscous dissipation Eq. (2.22) becomes

$$u\frac{\partial T}{\partial x} + v\frac{\partial T}{\partial y} = \frac{\mu_{nf}}{\rho_{nf}}\frac{\partial^2 T}{\partial y^2}. \tag{2.24}$$

The corresponding boundary conditions are

$$T = T_w \qquad \text{at } y = 0, \quad T \to T_\infty \qquad \text{as } y \to \infty.$$

In above expression α_{nf} display the nanofluid thermal diffusivity and k_{nf} express the nanofluid effective thermal conductivity. The Maxwell- Garnett's (Abu-Nada and Oztop [34]) model approximated the k_{nf} in the form are

$$\begin{aligned} (\rho C_p)_{nf} &= \frac{k_{nf}}{\alpha_{nf}}, \\ (\rho C_p)_{nf} &= \phi(\rho C_p)_s + (1-\phi)(\rho C_p)_f, \end{aligned} \tag{2.25}$$

$$k_{nf} = \frac{(k_s + 2k_f) - 2\phi(k_f - k_s)}{\phi(k_f - k_s) + (k_s + 2k_f)} k_f. \tag{2.26}$$

The thermal conductivity of base fluid and solid particles are symbolizing by k_f and k_s respectively, similarly the heat capacities of base fluid and solid particles are denoted with $(\rho C_p)_s$ and $(\rho C_p)_{nf}$.

2.3 Similarity transformation

The similarity transformation for the present problem are

$$\begin{aligned} &\psi = \sqrt{\left(\frac{2\upsilon_f x u_e(x)}{m+1}\right)} f(\eta), \qquad \eta = \sqrt{\left(\frac{(m+1)u_e(x)}{2\upsilon_f x}\right)} y, \\ &\theta = \frac{(T - T_\infty)}{(T_w - T_\infty)}. \end{aligned} \tag{2.27}$$

Here ψ represent the stream function and is characterized in the established way as $u = \partial\psi / \partial y$ and $v = -\partial\psi / \partial x$ to indistinguishably fulfill Eq. (2.1) and υ_f denoted the kinematic viscosity of the fluid. Now using above stream function, we get the form of *u* and *v* is

$$u = x^m U_\infty f'(\eta), \quad v = -\sqrt{\left(\frac{(m+1)U_\infty \upsilon_f x^m}{2}\right)}\left\{ f(\eta) + \eta\left(\frac{m-1}{m+1}\right) f'(\eta)\right\}. \tag{2.28}$$

Using transformations (2.27) and (2.28) in Eqs. (2.15) to (2.24) the following ordinary differential equation becomes

$$\frac{1}{(1-\phi)^{\frac{25}{10}}(1-\phi+\phi\frac{\rho_s}{\rho_f})} f''' + ff'' + (\tfrac{2m}{m+1})(1-f'^2) = 0, \tag{2.29}$$

$$\frac{1}{\Pr}\frac{k_{nf}/k_f}{[1-\phi+\phi\frac{(\rho C_p)_s}{(\rho C_p)_f}]}\theta'' + f\theta' = 0. \tag{2.30}$$

And the boundary conditions become

(i) Static wedge

$$\begin{aligned} &f'(0) = f(0) = 0, \ \theta(0) = 1 \\ &f'(\infty) = 1, \quad \theta(\infty) = 0\ . \end{aligned} \tag{2.31}$$

(ii) Moving wedge

$$\begin{aligned} &f'(0) = \lambda, \ f(0) = 0, \ \theta(0) = 1, \\ &f'(\infty) = 1, \quad \theta(\infty) = 0. \end{aligned} \tag{2.32}$$

In above equations prime indicate differentiation with respect to η, Pr validate the Prandtl number and the parameter β and λ respectively known as Hartee pressure gradient and moving wedge parameter is designated as

$$\beta_0 = \frac{2m}{(m+1)}, \quad \lambda = \frac{U_w}{U_\infty}, \quad \Pr = \frac{\upsilon_f}{\alpha_f}. \tag{2.33}$$

Here $\lambda=0$ resemble to a static wedge, while $\lambda > 0$ and $\lambda < 0$ respectively demonstrate the moving wedge in the same and inverse directions to the free stream. Moreover, Hartree pressure gradient parameter β_0 relates to $\Omega = \pi\beta_0$ for a wedge total angle Ω. Now positive estimation of β_0 measure the pressure gradient is good or negative, while is unfavorable for negative values of β_0, also β_0

=0 (Ω =0^o) illustrates the boundary layer flow past a horizontal flat plate, while β_0 = 1 (Ω =180^o) compares to the flow close to vertical flat plate and stagnation point. Further, when ϕ = 0 the present analysis reduces to that determined by Skan and Falkner [24] or Ishak et al [23].

2.4 Skin friction Coefficient

The skin friction coefficient is expressed as

$$C_f = \frac{\mu_{nf}\left(\partial u/\partial y\right)_{y=0}}{\rho_f u_e^{\,2}}. \tag{2.34}$$

Here $\mu_{nf}\left(\partial u/\partial y\right)_{y=0}$ indicate the shear stress of the surface operate the similarity transformation (2.25) in Eq. (2.32), we obtain

$$\left[2\,\mathrm{Re}_x/(m+1)\right]^{1/2} C_f = \frac{1}{(1-\phi)^{2.5}}\, f''(0), \tag{2.35}$$

where Re_x designate the local Reynolds number and it is defined as

$$\mathrm{Re}_x = \frac{u_e x}{\upsilon_f}. \tag{2.36}$$

2.5 Local Nusselt number

The local Nusselt number is define as

$$Nu_x = \frac{x q_w}{k_f\left(T_w - T_\infty\right)}, \tag{2.37}$$

in above equation q_w is heat flux of the surface that is defined as

$$q_w = -k_{nf}\left(\frac{\partial T}{\partial y}\right)_{y\to 0}. \tag{2.38}$$

Using Eq. (2.36) and similarity transformation (2.25) in Eq. (2.34), we get the form

$$\left[(m+1)\,\mathrm{Re}_x/2\right]^{-1/2} Nu_x = -\frac{k_{nf}}{k_f}\theta'(0). \tag{2.39}$$

2.6 Shooting Technique

Shooting technique is a technique in numerical analysis which help, in the solution of the initial value problem. Generally, we “shoot” out directions in various path until we catch the correct boundary value. The benefit of the shooting technique is that it exploits the speed and adaptivity of technique for initial value problems. The drawback of the technique is that it is not as powerful as collocation or finite difference methods, problem having initial condition with developing modes are inherently unstable even though the boundary value problem itself might be quite stable and posed.

Now to solve our problem with the help of the shooting technique we reduce the Eqs. (2.29) and (2.30) and its boundary condition (2.31) and (2.32) to first order by choosing some approximation i.e.

$$f(\eta) = h(1), \tag{2.40}$$

$$f'(\eta) = h(2), \tag{2.41}$$

$$f''(\eta) = h(3), \tag{2.42}$$

$$f'''(\eta) = \mathrm{F}(3) = -(1-\phi)^{2.5}\left(1-\phi+\phi\frac{\rho_s}{\rho_f}\right)\{h(1)h(3)+\frac{2m}{(m+1)}(1-h(2)^2)\}, \tag{2.43}$$

$$\theta(\eta) = h(4), \tag{2.44}$$

$$\theta'(\eta) = h(5), \tag{2.45}$$

$$\theta''(\eta) = \mathrm{F}(5) = -\mathrm{Pr}\frac{\left[1-\phi+\phi\dfrac{(\rho C_p)_s}{(\rho C_p)_f}\right]}{k_{nf}/k_f}h(1)h(5). \tag{2.46}$$

And its boundary conditions

(i) Static wedge

$$\begin{aligned} &h(1)=0, \quad h(2)=0, \quad h(4)=1, \quad \text{as} \quad \eta \to 0, \\ &h(2)=1, \quad h(4)=0, \quad \text{as} \quad \eta \to \infty. \end{aligned} \tag{2.47}$$

(ii) Moving wedge

$$\begin{aligned} &h(1)=0, \quad h(2)=\lambda, \quad h(4)=1, \quad \text{as} \quad \eta \to 0, \\ &h(2)=1, \quad h(4)=0, \quad \text{as} \quad \eta \to \infty. \end{aligned} \tag{2.48}$$

2.7 Result and discussion

Goal of this section is to demonstrate the influence of rising parameters heat transport phenomenon, velocity, and temperature profiles. Accordingly, the Figs. 2.2-2.9 have been constructed. Fig. 2.2 signify the effect of ϕ (solid volume friction) on the axial velocity. It is perceived that axial velocity increases for both static and moving wedge cases with enhancing the value of volume friction ϕ. The influence of volume friction ϕ on temperature field is portrayed in Fig. 2.3. It is noticed that the temperature field shows dual behavior for λ>-0.5, the temperature profile increases while for λ<-0.5 the temperature profile decreases for increasing value of volume friction ϕ. Fig. (2.4-2.5) depict the variation of velocity profile and temperature field for distinct value of Hartree pressure gradient parameter β_0. The axial velocity enhances for both static or moving wedge while temperature field shows inverse behavior for both moving and static wedge parameter for different value of β_0. Further, we can see that the boundary layer thickness thinning for moving wedge and it is thickening for static wedge parameter. Fig. 2.6 sketch the velocity profile for several values of moving wedge parameter λ. The velocity distribution enhances with increment in wedge parameter λ for both the cases i.e. flow past a flat plate and a

stagnation-point flow. Further, we noticed that the momentum boundary layer thickness is larger in the case of flow past a flat plate when compare with a stagnation-point flow. Fig. 2.7 reveal the impact of velocity ratio parameter λ on fluid temperature. For the flourishing values of the velocity ratio parameter λ, the temperature shows decreasing behavior in both case, i.e, flow past a flat plate and near the stagnation-point flow. The velocity distribution with the effect of nanoparticle have demonstrated in Fig. 2.8. It is shows that the Cu-water have more velocity distribution as compared to Al_2O_3, TiO_2. On the other hand, Cu-water have lowest fluid temperature field than Al_2O_3, TiO_2 is portrayed in Fig. 2.9. In both Fig. (2.8 and 2.9) we draw the graph for static and moving wedge and its maintain same behavior. Table 2.2 show the comparison value of $f''(0)$ with some other research papers such as Watanabe [32] and Yih [33]. Table (2.3) to (2.5) signify the magnitude of drag force and Nusselt number for different nanoparticle such as Cu, Al_2O_3 and TiO_2 respectively. Now increases the value of wedge parameter and m the magnitude of drag force and Nusselt number increases.

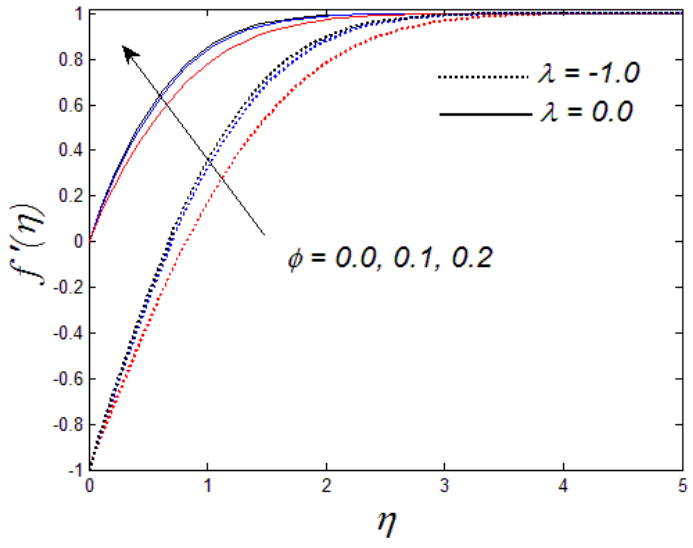

Fig. 2.2 Effect of ϕ (volume friction) on $f'(\eta)$ when $m=1$ and $\Pr=6.2$.

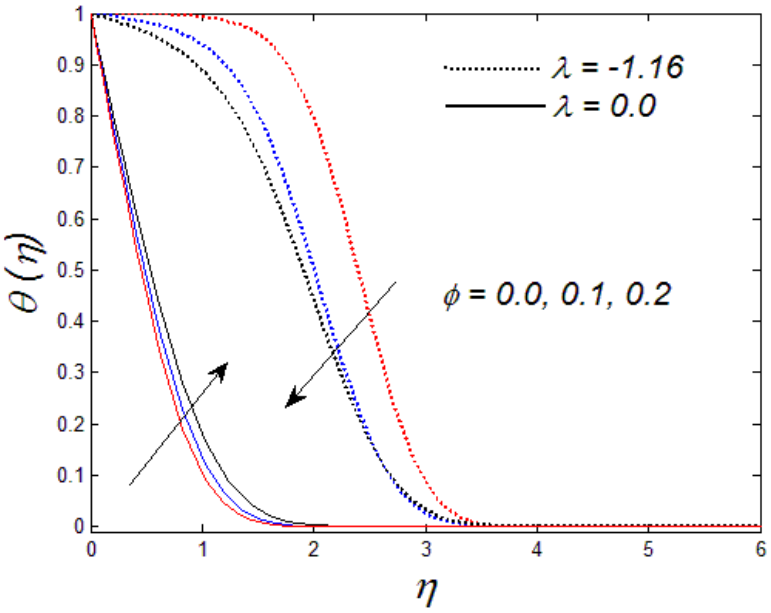

Fig. 2.3 Effect of volume friction ϕ on $\theta(\eta)$ when $m=1$ and $\Pr=6.2$.

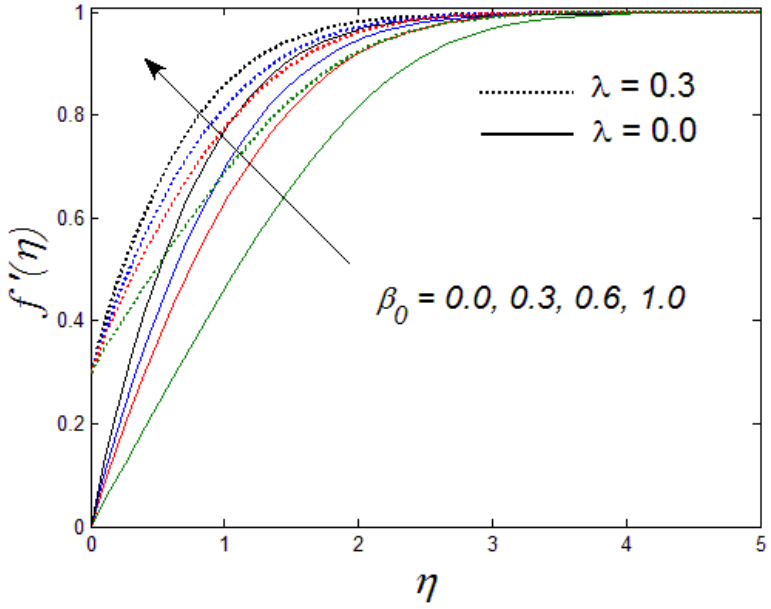

Fig. 2.4 Effect of Hartree pressure gradient parameter β_0 on $f'(\eta)$ when $\Pr=6.2$ and $\phi=0.1$

.

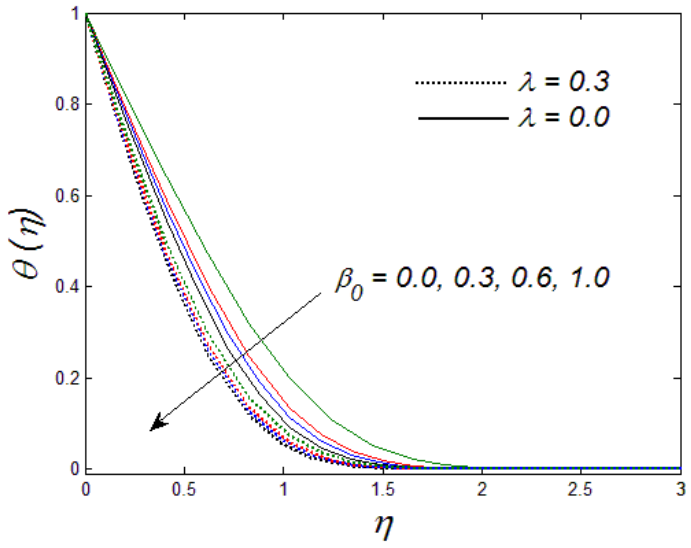

Fig. 2.5 Effect of Hartree pressure gradient parameter β_0 on $\theta(\eta)$ when $\Pr = 6.2$ and $\phi = 0.1$.

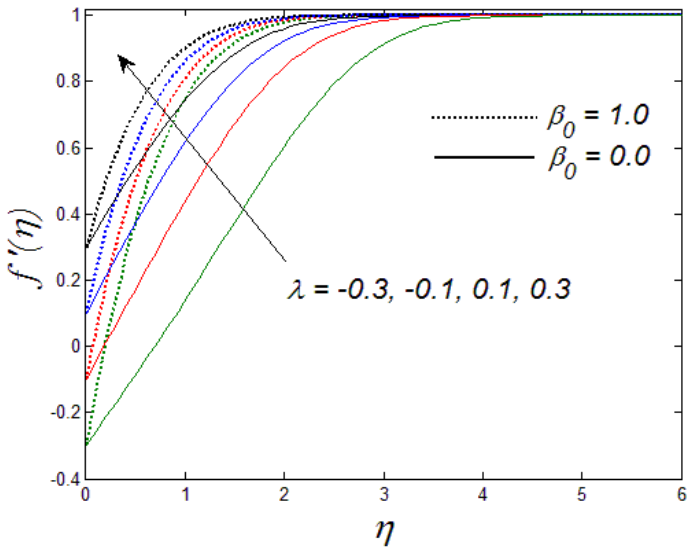

Fig. 2.6 Effect of wedge parameter λ on $f'(\eta)$ when $\Pr = 6.2$ and $\phi = 0.1$.

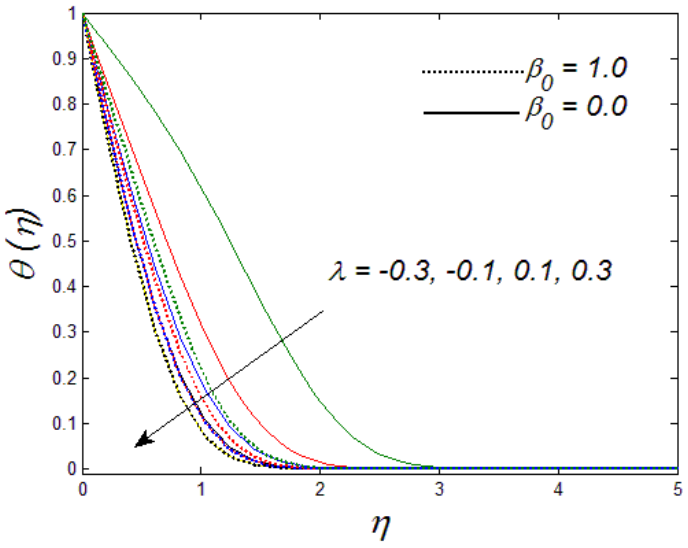

Fig. 2.7 Influence of wedge parameter λ on $\theta(\eta)$ when $\Pr = 6.2$ and $\phi = 0.1$.

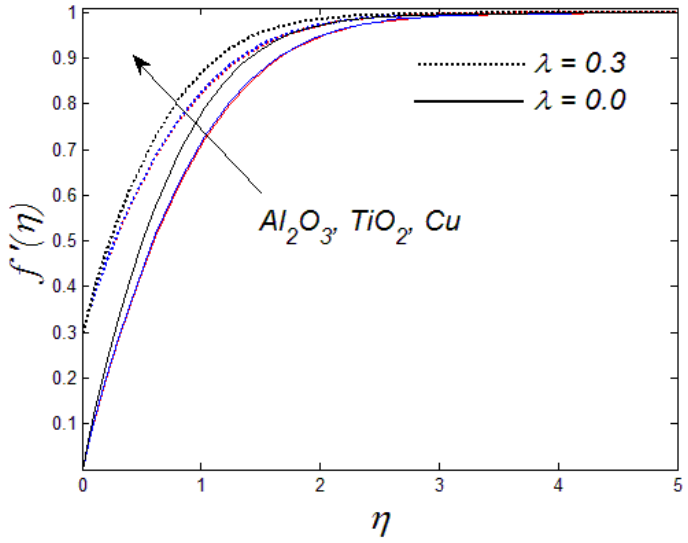

Fig. 2.8 Effect of different nanoparticle on $f'(\eta)$ when $\Pr = 6.2$, $m = 0.5$ and $\phi = 0.1$.

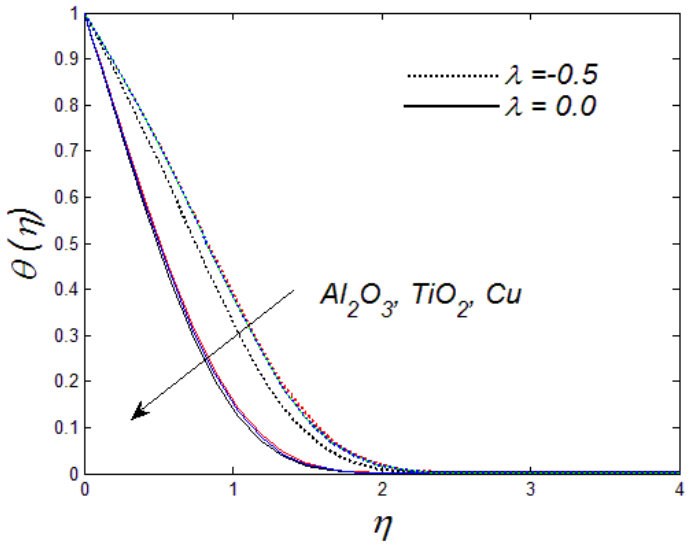

Fig. 2.9: Effect of different nanoparticle on $\theta(\eta)$ when $\Pr = 6.2$, $m = 0.5$ and $\phi = 0.1$.

m	Watanabe [32]	Yih [33]	Present result
0	0.46960	0.469600	0.4696
1/11	0.65498	0.654979	0.6550
0.2	0.80213	0.802125	0.8021
1/3	0.92765	0.927653	0.9277
0.4	-	-	-
0.5	-	-	1.0389
1	-	1.232588	1.2326

Table 2.2: comparison analysis of $f''(0)$ for certain values of m with λ =0, ϕ =0.0.

m	ϕ	$\frac{1}{(1-\varphi)^{2.5}} f''(0)$	$-\frac{k_{nf}}{k_f} \theta'(0)$
0	0.1	0.7179	1.1100
	0.2	0.9992	1.3342
0.5	0.1	1.5881	1.3472
	0.2	2.2105	1.6048
1	0.1	1.8843	1.4043
	0.2	2.6226	1.6692

Table 2.3: show the wall shear stress and heat transfer for Cu, when λ =0 and certain values of m and ϕ.

m	ϕ	$\frac{1}{(1-\varphi)^{2.5}} f''(0)$	$-\frac{k_{nf}}{k_f} \theta'(0)$
0	0.1	0.6103	1.0423
	0.2	0.7842	1.2092
0.5	0.1	1.3502	1.2744
	0.2	1.7348	1.4718
1	0.1	1.6019	1.3305
	0.2	2.0584	1.5352

Table 2.4: show the wall shear stress and heat transfer for Al_2O_3, when λ =0 and various values of m and ϕ.

m	ϕ	$\frac{1}{(1-\varphi)^{2.5}} f''(0)$	$-\frac{k_{nf}}{k_f} \theta'(0)$
0	0.1	0.6169	1.0189
	0.2	0.7978	1.1561
0.5	0.1	1.3648	1.2460
	0.2	1.7651	1.4082
1	0.1	1.6192	1.3010
	0.2	2.0942	1.4691

Table 2.5: show the wall shear stress and heat transfer for TiO_2, when λ =0 and different values of m and ϕ.

2.8 Concluding Remarks

The effect of moving wedge and static wedge on the Falkner-Skan flow has been investigated. Finally, the numerical solution is obtained with the help of shooting technique from MATLAB. The main key point of the present analysis is as follow.

- The velocity profile enhances with the increment of volume friction ϕ.
- The temperature profile shows dual behavior with the increase of ϕ parameter.
- Cu/water have enhanced velocity profile than Al_2O_3, and TiO_2 and reverse behavior occur for temperature profile.
- For various value of wedge parameter λ the axial velocity increases while temperature field decrease.

Chapter 3

Falkner-Skan problem in the flow of a nanofluids in presence of induced magnetic field

3.1 Introduction

This chapter consists of the numerical solution for Falkner-Skan flow of a static and moving wedge flow. The characteristics of induced magnetic field are incorporated in a viscous fluid. Heat flux is evaluated through the Fourier's law of heat conduction. The boundary value problem is solved numerically with the help of shooting technique coupled with Runge-Kutta and Newton's method. Three distinct types of nanoparticles, Cu, Al_2O_3, and TiO_2 are studied with water used as base fluid. The impacts of sundry parameters, i.e velocity ratio parameter, wedge angle parameter, and solid volume friction on the velocity distribution, induced magnetic field and temperature field are presented. An excellent agreement is found with available result in the absence of body forces.

3.2 Theory and flow analysis

The geometry for the flow frame work is identified in Fig. 3.1. An incompressible, two-dimensional steady flow of a nanofluid past a moving and static wedge is incorporated. The influence of the induced magnetic field is considered. Table. 3.1 characterized the thermophysical properties of solid particle and fluid. Moreover, the velocity of the ambient fluid and moving wedge flow are $u(x) = U_\infty x^m$ and $u_w(x) = U_w x^m$ are assumed respectively, where U_∞, U_w, and m are constant with $0 \le m \le 1$. Incorporating the boundary layer approximation, the fundamental equations of conservation of velocity and momentum, induced magnetic and temperature fields with no viscous dissipation can be declared as

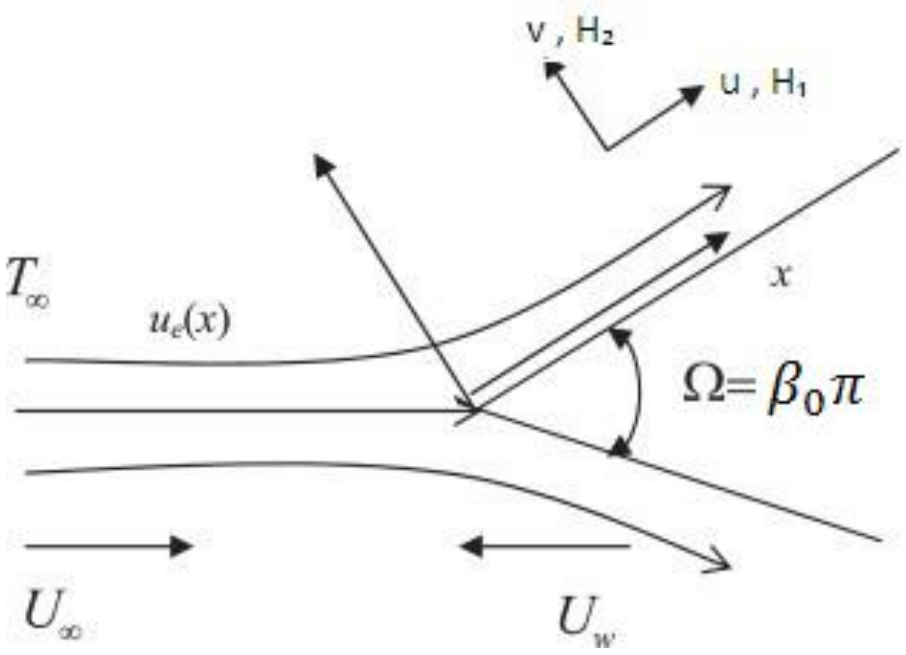

Fig. 3.1 Physical flow chart and coordinate system.

$$\frac{\partial u}{\partial x} + \frac{\partial v}{\partial y} = 0, \tag{3.1}$$

$$\frac{\partial H_1}{\partial x}+\frac{\partial H_2}{\partial y}=0, \tag{3.2}$$

$$u\frac{\partial u}{\partial x}+v\frac{\partial u}{\partial y}-\frac{\mu}{4\pi\rho_f}(H_2\frac{\partial H_1}{\partial y}+H_1\frac{\partial H_1}{\partial x})=(u_e\frac{du_e}{dx}-\frac{\mu H_e}{4\pi\rho_f}\frac{dH_e}{dx})+\frac{\mu_{nf}}{\rho_{nf}}\frac{\partial^2 u}{\partial y^2}, \tag{3.3}$$

$$u\frac{\partial H_1}{\partial x}+v\frac{\partial H_1}{\partial y}-H_2\frac{\partial u}{\partial y}-H_1\frac{\partial u}{\partial x}=\mu_e\frac{\partial^2 H_1}{\partial y^2}, \tag{3.4}$$

$$u\frac{\partial T}{\partial x}+v\frac{\partial T}{\partial y}=\frac{\mu_{nf}}{\rho_{nf}}\frac{\partial^2 T}{\partial y^2}. \tag{3.5}$$

The suitable boundary conditions are given by:

i) Static wedge

$$\begin{aligned}
&v\big|_{y=0}=0, \qquad u\big|_{y=0}=0, \qquad T\big|_{y=0}=T_w,\\
&\left.\frac{\partial H_1}{\partial y}\right|_{y=0}=H_2\big|_{y=0}=0,\\
&u\big|_{y\to\infty}\to u_e(x)=U_\infty x^m, \qquad T\big|_{y\to\infty}\to T_\infty,\\
&H_1\big|_{y\to\infty}\to H_e(x)=H_0x^m.
\end{aligned} \tag{3.6}$$

ii) Moving wedge

$$\begin{aligned}
&v\big|_{y=0}=0, \quad u\big|_{y=0}=u_w(x)=U_w x^m, \quad T\big|_{y=0}=T_w,\\
&\left.\frac{\partial H_1}{\partial y}\right|_{y=0}=H_2\big|_{y=0}=0,\\
&u\big|_{y\to\infty}\to u_e(x)=U_\infty x^m, \qquad T\big|_{y\to\infty}\to T_\infty,\\
&H_1\big|_{y\to\infty}\to H_e(x)=H_0x^m.
\end{aligned} \tag{3.7}$$

Here x and y are, respectively, the separation towards the sheet of the wedge and normal to wedge; the velocity components through (x, y) are taken to by (u, v) respectively. (H_1, H_2) symbolizes the

components of induced magnetic field. Where $H_e(x)$ and $u_e(x)$ are the x component of magnetic field and velocity, H_0 is the applied magnetic field parallel to plate in free stream, T delineate the fluid temperature, ρ_f, μ, σ, $\mu_e = 1/4\pi\sigma\mu$, is the density of fluid, magnetic permeability, electric conductivity, and magnetic diffusivity, respectively, viscosity of the nanofluid is identified μ_{nf}, α_{nf} signify the thermal diffusivity, and ρ_{nf} exemplify the density of the nanofluid. The numerical values of the specific heat, density, and thermal conductivity, are listed in the Table. 3.1 for both nanofluid and regular fluid.

Thermo-Physical properties	Fluid phase (water)	Cu	Al_2O_3	TiO_2
$\propto \times 10^{-7}(m^2/s)$	1.470	1163.10	131.70	30.70
ρ (kg/m^3)	997.10	8933.0	3970.0	4250.0
C_p(J/K.kg)	4179.0	385.0	765.0	686.20
K(W/mK)	0.6130	400.0	40.0	8.95380

Table 3.1: The thermophysical properties of the solid particle and base fluid.

The mathematical expression for the thermophysical properties are

$$
\begin{aligned}
&(\rho C_p)_{nf} = \frac{k_{nf}}{\alpha_{nf}}, \qquad \frac{\mu_{nf}}{\mu_f} = \frac{1}{(1-\phi)^{25/10}} \\
&(\rho C_p)_{nf} = \phi(\rho C_p)_s + (1-\phi)(\rho C_p)_f, \\
&k_{nf} = \frac{(k_s + 2k_f) - 2\phi(k_f - k_s)}{\phi(k_f - k_s) + (k_s + 2k_f)} k_f .
\end{aligned}
\tag{3.8}
$$

In above parameter, ϕ characterize the solid volume friction, μ_f demonstrate the modified viscosity of the base fluid, ρ_f and ρ_s are the densities of the regular fluid and solid particle,

$(\rho C_p)_{nf}$ signify the effective heat capacity of the nanofluid, $(\rho C_p)_f$ and $(\rho C_p)_s$ are the heat capacity of the base fluid and solid particle respectively, k_{nf} perceive the modified thermal conductivity of the nanofluid, k_f and k_s are the respective thermal conductivity of the base fluid and solid particle.

3.3 Similarity transformation

Now we are applying the following transformation to reduce the two independent variables to one and the fundamental equations become dimensionless, i.e.

$$\begin{aligned}
&\psi = \sqrt{\frac{2\nu_f\ x u_e(x)}{(m+1)}}\, f(\eta),\ \eta = \sqrt{\frac{(m+1)u_e(x)}{2x\nu_f}}\, y,\ u = U_\infty x^m f'(\eta),\\
&v = -\sqrt{\frac{U_\infty (m+1)x^{m-1}\nu_f}{2}}\left\{ f(\eta) + \eta\left(\frac{m-1}{m+1}\right) f'(\eta)\right\}, H_1 = H_0 x^m g'(\eta),\\
&H_2 = -H_0\sqrt{\frac{2x^{m-1}\nu_f}{U_\infty (m+1)}}\left\{ mg(\eta) + \eta\left(\frac{m-1}{2}\right) g'(\eta)\right\}, \theta(\eta) = \frac{T-T_\infty}{T_w - T_\infty}.
\end{aligned} \tag{3.9}$$

Eqs. (3.1) and (3.2) are fulfilled indistinguishable, and Eqs. (3.3) to (3.5) get to be

$$\frac{1}{(1-\phi)^{2.5}(1-\phi+\phi\frac{\rho_s}{\rho_f})} f''' + ff'' + \left(\frac{2m}{m+1}\right)(1-f'^2) + \beta(mg'^2 - mgg'' - m) = 0, \tag{3.10}$$

$$Mg''' + fg'' - \left(\frac{2m}{m+1}\right) gf'' = 0, \tag{3.11}$$

$$\frac{\frac{k_{nf}}{k_f}}{p_r[1-\phi+\phi\frac{(\rho C_p)_s}{(\rho C_p)_f}]}\theta'' + f\theta' = 0. \tag{3.12}$$

What's more the boundary conditions (3.6) and (3.7) take the accompanying structure

i) Static wedge

$$f(\eta) = f'(\eta) = 0,\ \theta(\eta) = 1,\ g(\eta) = g''(\eta) = 0,\ \eta = 0, \tag{3.13}$$

$$f'(\eta)=1,\ \theta(\eta)=0,\ g'(\eta)=1,\ \eta\to\infty.$$

ii) Moving wedge

$$f'(\eta)=\lambda,\ \ f(\eta)=0,\ \theta(\eta)=1,\ g''(\eta)=g(\eta)=0,\quad \eta=0,$$

$$f'(\eta)=1,\ \theta(\eta)=0,\ g'(\eta)=1,\ \eta\to\infty. \tag{3.14}$$

In above equation prime indicate the derivative with respect to η. The parameters of λ is the consistent moving wedge parameter with $\lambda > 0$ and $\lambda < 0$ relate to a moving wedge in the same and inverse direction to the free stream, individually, while $\lambda = 0$ compares to a static wedge , β (is the magnetic parameter), *M* (reciprocal magnetic Prandtl number) and Pr (Prandtl number) are as follows

$$\lambda=\frac{U_w}{U_\infty},\ \beta=\frac{\mu_e H_0^2}{4\pi\rho {U_\infty}^2},\ M=\frac{\mu_e}{\nu_f}=\frac{1}{4\pi\sigma\mu\nu_f},\ p_r=\frac{\nu_f}{\alpha_f},$$

It might be noticed that for β (in absence of magnetic field), Eq. (3.10) reduce to that of Ishak [27]. Since β =0 suggest the non-appearance of the magnetic field, Eq. (3.11) governing the induced magnetic field is did not require anymore. Moreover, consider $\beta_0=\frac{2m}{m+1}$ describe the Hartee pressure gradient parameter which relates to $\beta_0=\Omega/\pi$ for a complete angle Ω of the wedge. As indicated by white [34], positive value of β_0 manner the pressure gradient is negative or favorable and negative value of β_0 denotes an unfavorable pressure gradient. Moreover β_0 =1 ($\Omega=180^\circ$) and β_0 =0 ($\Omega=0^\circ$) are the respective boundary layer flow past a horizontal flat plate and near the stagnation point of a vertical flat plate.

The physical quantities of intrigue are the wall shear stress C_f and the local Nusselt number Nu_x,

which are characterized as,

$$C_f = \frac{\tau_w}{\rho_f u_e^2},\ Nu_x = \frac{xq_w}{(T_w - T_\infty)k_f}, \tag{3.15}$$

Here the surface heat flux q_w and surface shear stress τ_w are given by

$$\tau_w = \mu_{nf} \left.\frac{\partial u}{\partial y}\right|_{y=o}, \quad q_w = -k_{nf} \left.\frac{\partial T}{\partial y}\right|_{y=0}. \tag{3.16}$$

Using Eq. (9) and (16), in Eq. (15) we obtain

$$[2\,\mathrm{Re}_x/(m+1)]^{1/2} C_f = \frac{1}{(1-\varphi)^{\frac{25}{10}}} f''(0),\ \ [\mathrm{Re}_x(m+1)/2]^{-1/2} Nu_x = -\frac{k_{nf}}{k_f}\theta'(0). \tag{3.17}$$

3.4 Numerical method and evidence

The ordinary differential equations (3.10) to (3.12) under the boundary conditions and initial condition (3.13) will be solved with the help of shooting technique. In this method, first we change over the third order ordinary differential equations to first order, and have picked a reasonable finite value of η_∞, say η_∞, and absolute convergence criteria were taken as 10^{-6}, we set the following first order systems,

$$f' = p,\ \ f'' = q, \tag{3.18}$$

$$q' = f''' = -(1-\varphi)^{\frac{25}{10}}\left(1-\varphi+\varphi\frac{\rho_s}{\rho_f}\right)\left\{qf + \frac{2m}{(m+1)}(1-f'^2)\right\}, \tag{3.19}$$

$$g' = r, r' = s, \tag{3.20}$$

$$s' = g''' = -\frac{1}{M}\left\{ fs - (\frac{2m}{m+1})gq \right\}, \tag{3.21}$$

$$\theta' = t \tag{3.22}$$

$$t' = \theta'' = -\frac{p_r[1-\varphi+\varphi\frac{(\rho C_p)_s}{(\rho C_p)_f}]}{\frac{k_{nf}}{k_f}} f\theta', \tag{3.23}$$

with the conditions,

$$p(\eta) = \lambda,\ f(\eta) = 0,\ \theta(\eta) = 1,\ g(\eta) = 0, s(\eta) = 0,\ \eta = 0, \tag{3.24a}$$

$$p(\eta) = 1,\ \theta(\eta) = 0,\ r(\eta) = 1,\ \eta \to \infty, \tag{3.24b}$$

In this method, the decision of η_∞=10, guarantees that every numerical solution approach asymptotic values accurately. The present result for different values of *m* in the absence of induced magnetic field effects are contrasted and those reported by Watanabe [32], Yih [33], and Yacob [27] in Table 3.2. It is seen that the correlation demonstrates great understanding for every consider value, hence, we are certain that the present result is right and precise.

m	Watanabe [32]	Yih [33]	Yacob [27]	Present result
0	0.46960	0.469600	0.4696	0.469600
1/11	0.65498	0.654979	0.6550	0.654994
0.2	0.80213	0.802125	0.8021	0.802125
1/3	0.92765	0.927653	0.9277	0.927680
0.4	-	-	-	0.976824
0.5	-	-	1.0389	1.038900
1	-	1.232588	1.2326	1.232587

Table 3.2: comparison of $f''(0)$ for various values of m with λ =0, ϕ =0.0, M=0 (in the absence of β)

3.5 Results and discussion

The boundary layer nanofluid flow past a static and moving wedge has been examined numerically. The impact of induced magnetic field is also incorporated. In present analysis, the water is utilized as a base fluid of the nanofluid. The thermos-physical behavior of the base fluid and nanofluid are given in Table 3.1. For base fluid (water) the specific Pr (Prandtl number) 6.2 are used. Then the impact of emerging parameters on the axial velocity, induced magnetic and temperature distribution are analyzed and talked about in detail. Moreover, numerical values of the drag force coefficient and Nusselt number for different nanoparticle are introduced in table (3.3) to (3.5).

ϕ	β	m	M	$\frac{1}{(1-\varphi)^{2.5}} f''(0)$	$-\frac{k_{nf}}{k_f} \theta'(0)$
0	0.2	0	10	0.46960	0.87692
0.1				0.71788	1.11009
0.2				0.99924	1.33426
0.1	0	0.5	10	1.58811	1.34735
	0.1			1.56794	1.34176
	0.2			1.54699	1.33590
0.2	0.1	0	10	0.99924	1.33426
		0.5		2.18314	1.59844
		1		2.56554	1.65734
0.1	0.1	1	100	1.87595	1.40235
			1000	1.88337	1.40408
			5000	1.88402	1.40435

Table 3.3: The estimation of $\sqrt{2\mathrm{Re}_x/(m+1)}\ C_f$ and $[\mathrm{Re}_x(m+1)/2]^{-1/2} Nu_x$ for Cu, when λ =0 and various values for some parameter.

ϕ	β	m	M	$\frac{1}{(1-\varphi)^{2.5}} f''(0)$	$-\frac{k_{nf}}{k_f} \theta'(0)$
0	0.2	0	10	0.46960	0.87692
0.1				0.61034	1.05395
0.2				0.78420	1.23544
0.1	0	0.5	10	1.35023	1.28861
	0.1			1.33123	1.28269
	0.2			1.31145	1.27647
0.2	0.1	0	10	0.78420	1.23544
		0.5		1.70974	1.49672
		1		2.00600	1.55534
0.1	0.1	1	100	1.59396	1.34323
			1000	1.60112	1.34522
			5000	1.60177	1.34536

Table 3.4: The estimations of $\sqrt{2\mathrm{Re}_x/(m+1)}\ C_f$ and $[\mathrm{Re}_x(m+1)/2]^{-1/2} Nu_x$ for Al_2O_3, when λ =0 and various values for some parameter.

ϕ	β	m	M	$\frac{1}{(1-\varphi)^{2.5}} f''(0)$	$-\frac{k_{nf}}{k_f} \theta'(0)$
0	0.2	0	10	0.46960	0.87692
0.1				0.61691	1.07021
0.2				0.79788	1.27091
0.1	0	0.5	10	1.36480	1.30888
	0.1			1.34567	1.30290
	0.2			1.32576	1.29662
0.2	0.1	0	10	0.79788	1.27091
		0.5		1.73984	1.54090
		1		2.04164	1.60158
0.1	0.1	1	100	1.61114	1.36440
			1000	1.61830	1.36640
			5000	1.61908	1.36666

Table 3.5: The estimation of $\sqrt{2\mathrm{Re}_x/(m+1)}\ C_f$ and $[\mathrm{Re}_x(m+1)/2]^{-1/2} Nu_x$ for TiO_2, when λ =0 and various values for some parameter.

The wall shear stress and Nusselt number are constructed in Tables (3.3) – (3.5). It is observed that an enhances in the nanoparticles volume fraction, rests in the heat transfer rate at the surface. Now the variety β of wall shear stress coefficient and the heat transfer coefficient for the settled estimation of some parameters discuss in above tables. We watched that drag force coefficient diminishes with the expansion of the magnetic parameter β. The explanation behind such a behavior is that the thermal boundary layer thickness turns out to broad as the β increases, which bring out lower temperature gradient at the surface, hence lower heat transfer at the surface.

Nonetheless, the impact of M on the heat transfer rate and skin friction coefficient is the same, as appeared in above tables for all nanoparticles, i.e. drag force coefficient and the heat transfer rate increment, and similar result is found for the parameter m.

Figs. (3.2) - (3.4) display the change of the velocity profile, induced magnetic profile, and temperature distribution for distinct values of β (magnetic parameter) when *M=1*, *m=0.5*, and ϕ *=0.1* are fixed, respectively, it can be seen that the velocity distribution and induced magnetic profile diminishes, while temperature increases with enhancing the estimation of β. Now the boundary layer thickness for static wedge is larger as compared to moving wedge.

Figs. (3.5) - (3.7) delineate the graph of velocity profile, induced magnetic profile, and temperature profile for Cu/water nanofluid when ϕ varies, respectively. We have perceive that as the values of the nanoparticles solid volume fraction (ϕ) increase, the velocity and induced magnetic profile increases while the temperature profile show different effect for different value of λ when their values is taken greater than -0.5 the temperature field increases while it is a dual behavior for the moving wedge range $-0.6 < \lambda < -1$ and temperature field decrease for $\lambda > -1$. The value assigns to remaining parameter is $m = 0.5$, $M = 1$, and $\beta = 0.04$.

Figs. (3.8) demonstrates the impact of *M* (reciprocal magnetic Prandtl number) on the induced magnetic field for Cu/water nanofluid. As *M* increases and $m=0.5$, $\beta = 0.04$, and $\phi = 0.1$ are settled, the induced magnetic field increases.

Figs. (3.9) - (3.11) justify the effect of β_0 on velocity distribution, temperature profile, and induced magnetic profile for Cu/water nanofluid films. It is found that the axial velocity increase, induced magnetic field and temperature distribution decrease for increasing the value of *m*, with $\phi = 0.1$, $\lambda = -0.4$, $\beta = 0.1$, and *M=1*. It is also noticed that from Fig. 9 shows that the boundary layer

thickness becomes thinner for moving wedge and then become higher for static wedge.

Figs. (3.12) - (3.14) presented the effect of different types of nanofluid for fixed value of ϕ=0.1, λ=-0.4, β=0.04, *M=1* and *m=0.5*. It is found that the Cu has high velocity distribution and induced magnetic field than TiO_2, Al_2O_3, while the opposite trend occurs for temperature profile.

Figs. (3.15) - (3.17) manifest the velocity profile, induced magnetic profile and temperature profile for various value of velocity ratio parameter λ. These figures are bestowed for two different value of β, especially, β = 0.0 (means flow past a flat plate) and β = 1.0 relate to a stagnation point flow. We noticed that for both case the induced magnetic profile and velocity profile increases while temperature field diminishes. Also, the boundary layer thickness is thinner in case of stagnation point flow is compared to the flow past a flat plate. All the figures fulfill the far field boundary conditions (3.24a) and (3.24b) asymptotically, in this manner bolster the validity of the numerical result got.

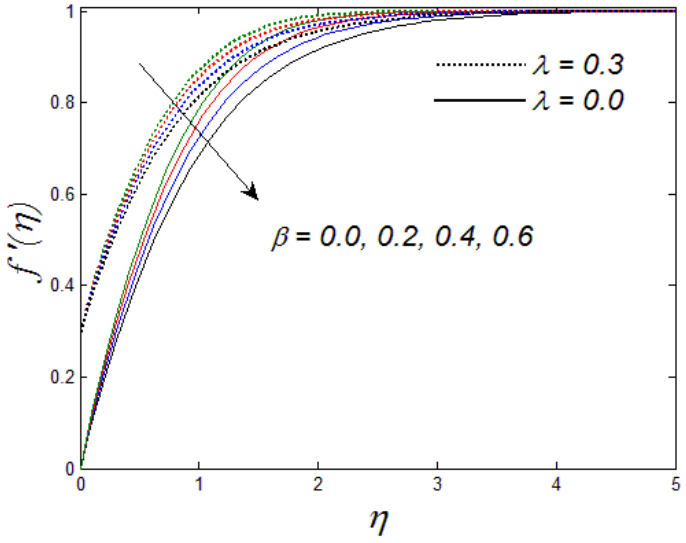

Fig. 3.2: Impact of β (magnetic parameter) on $f'(\eta)$.

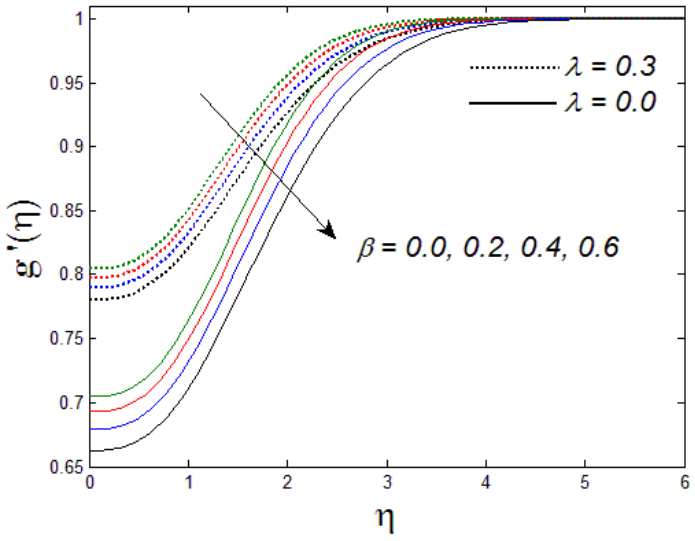

Fig. 3.3: Effect of β on induced magnetic profile $g'(\eta)$.

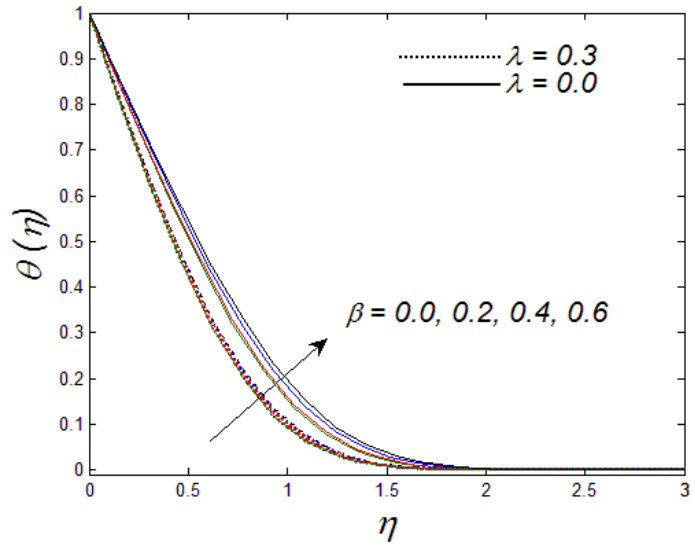

Fig. 3.4: Effect of β on temperature field $\theta(\eta)$.

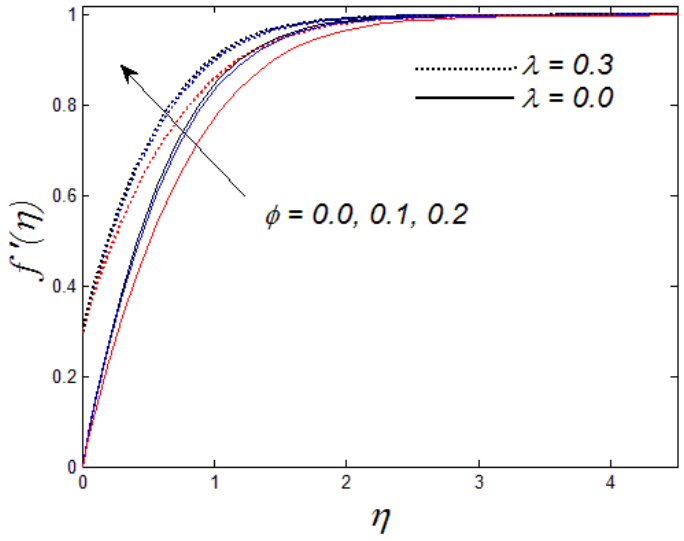

Fig. 3.5: Effect of solid volume friction (ϕ) on $f'(\eta)$.

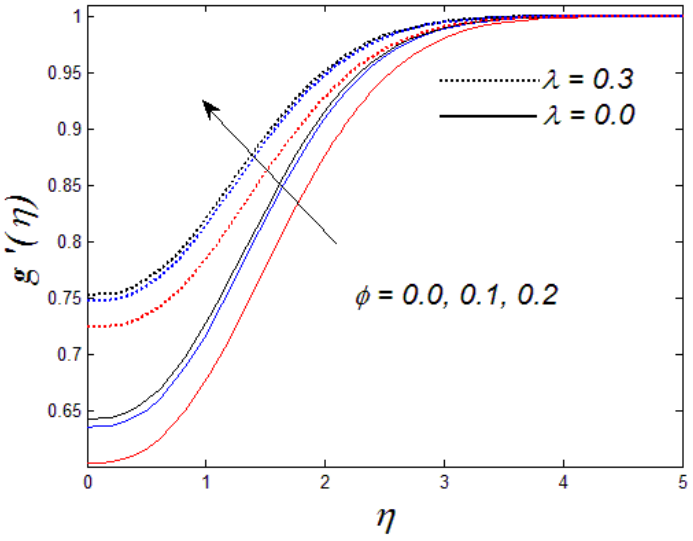

Fig. 3.6: Impact of solid volume friction (ϕ) on induced magnetic profile $g'(\eta)$.

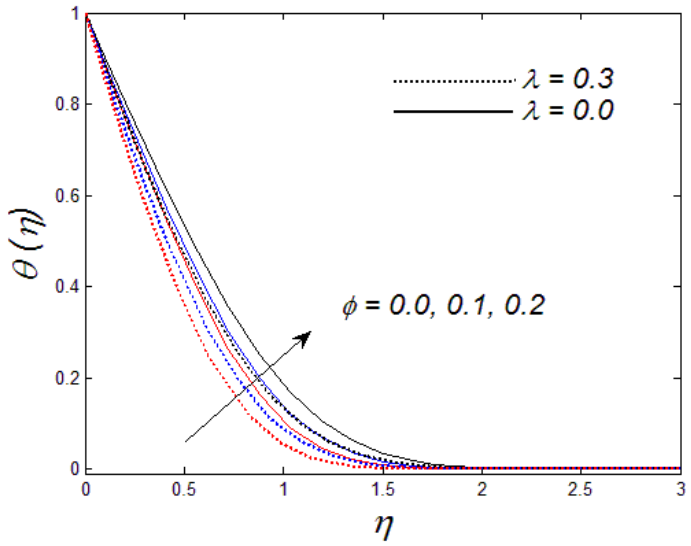

Fig. 3.7: Influence of solid volume friction (ϕ) on temperature distribution $\theta(\eta)$.

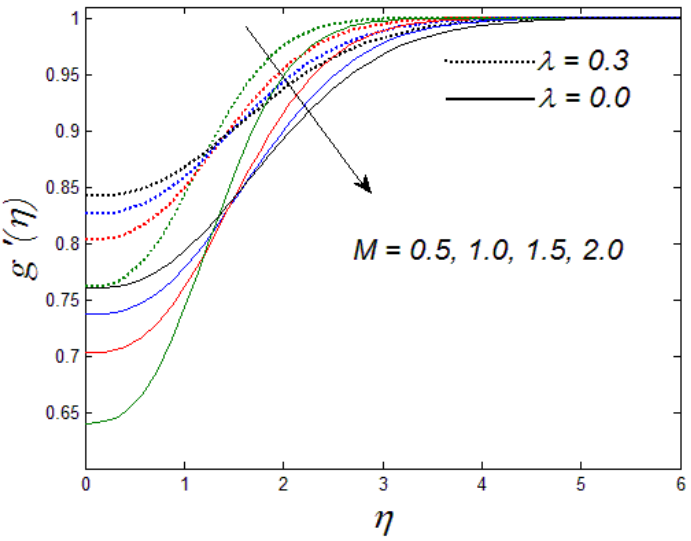

Fig. 3.8: Impact of M on induced magnetic profile $g'(\eta)$.

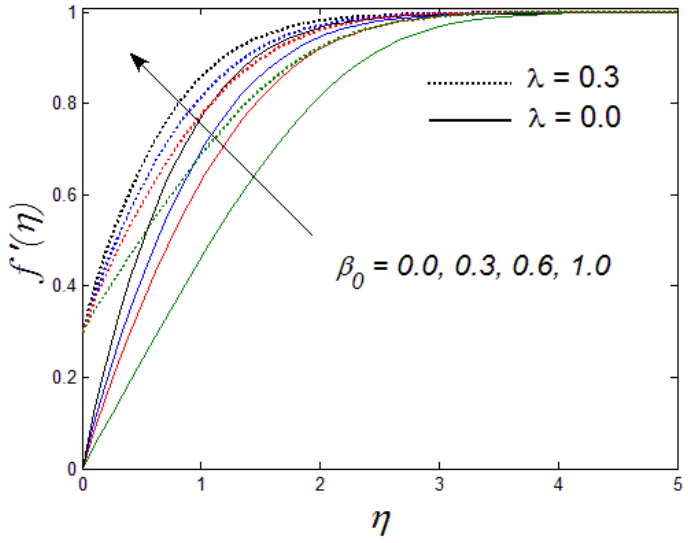

Fig. 3.9: Effect of pressure gradient parameter β_0 on $f'(\eta)$.

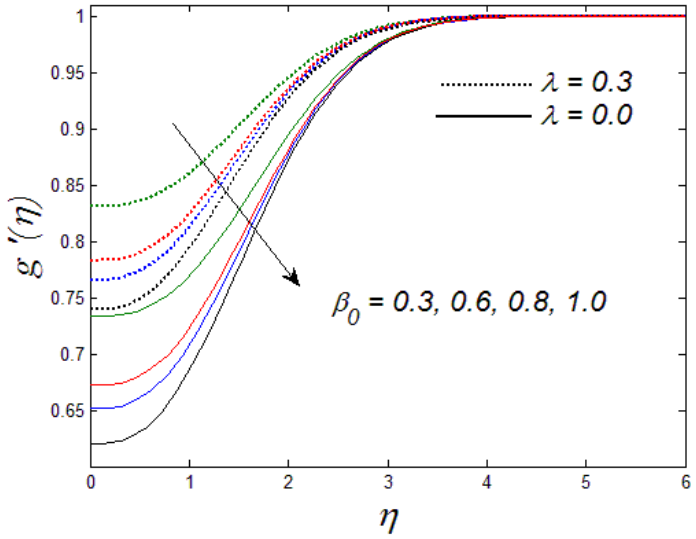

Fig. 3.10: Impact of pressure gradient parameter β_0 on $g'(\eta)$.

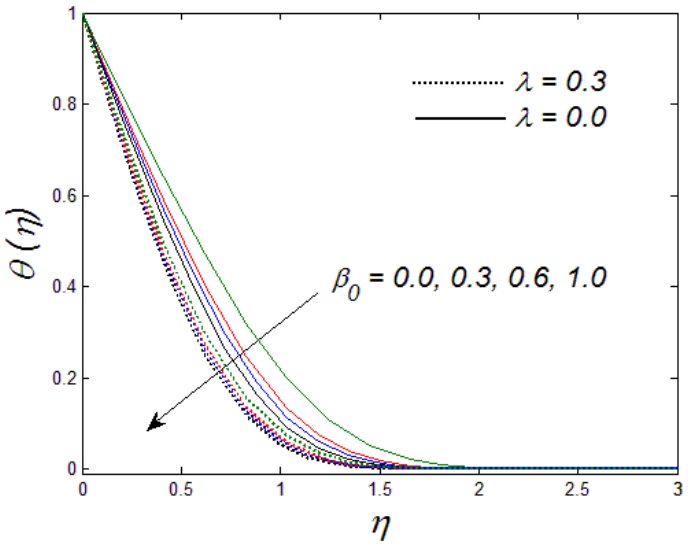

Fig. 3.11: Impact of wedge angle parameter (β_0) on temperature field $\theta(\eta)$.

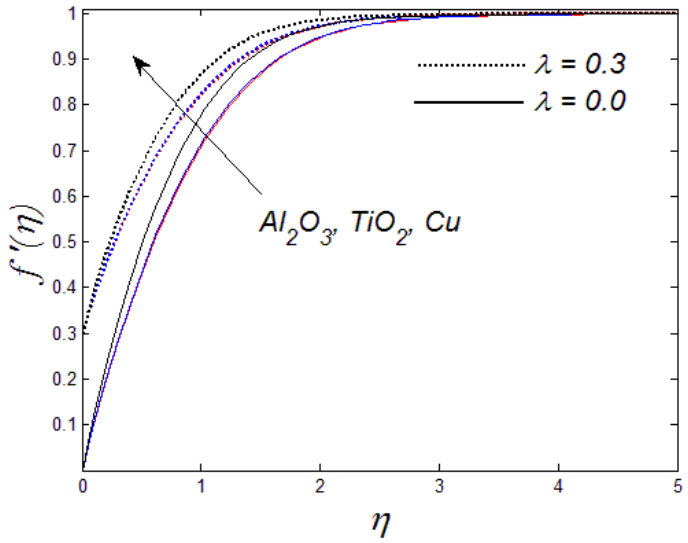

Fig. 3.12: Effect of nanoparticle on $f'(\eta)$.

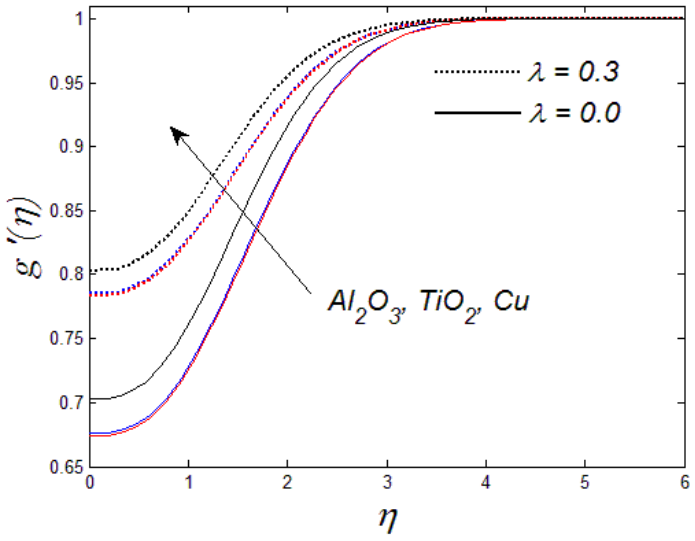

Fig. 3.13: Influence of nanoparticle on $g'(\eta)$.

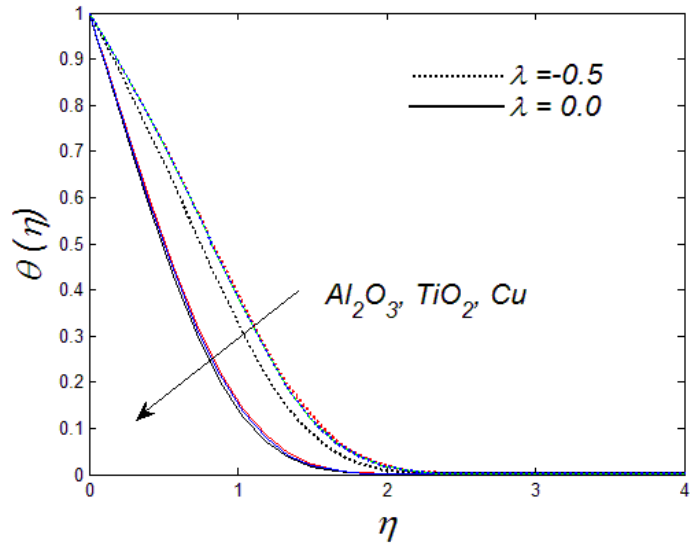

Fig. 3.14: Impact of nanoparticles on temperature field $\theta(\eta)$.

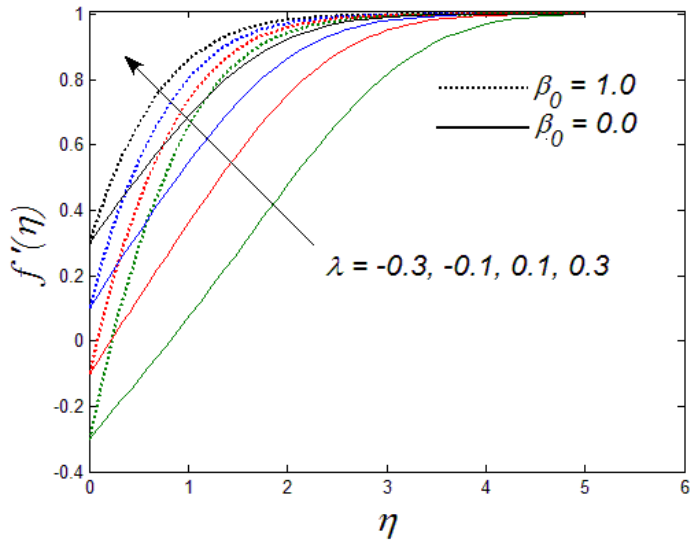

Fig. 3.15: Effect of wedge parameter λ on velocity profile $f'(\eta)$.

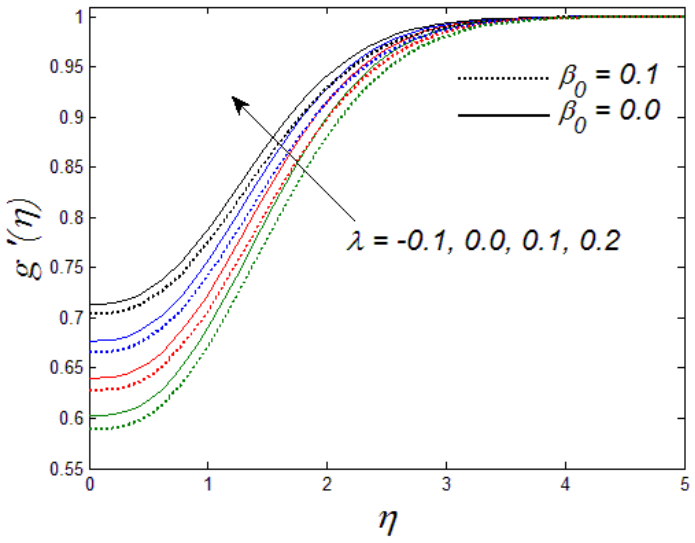

Fig. 3.16: Influence of wedge parameter λ on $g'(\eta)$.

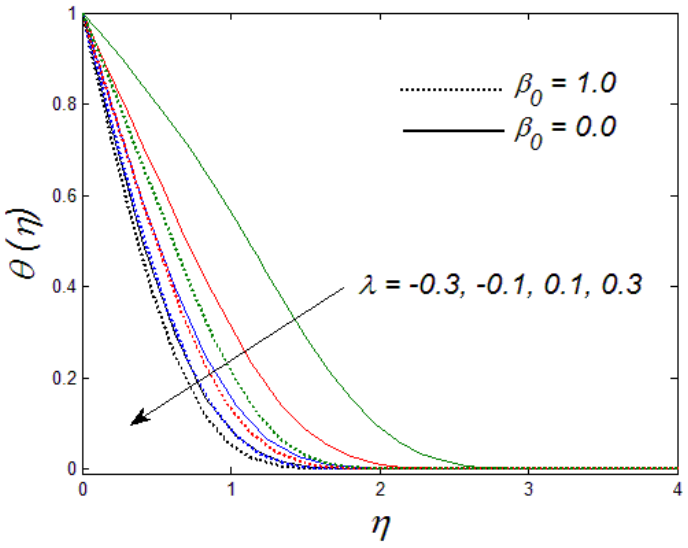

Fig. 3.17: Effect of wedge parameter λ on temperature field $\theta(\eta)$.

3.6 Concluding Comments

The Falkner-Skan problem for a moving and static wedge saturated in nanofluids with induced magnetic field is incorporated. The transformed equation resolved numerically by utilizing the Runge-Kutta technique. Three distinct sorts of nanoparticles, to be specific alumina Al_2O_3, copper Cu and titania TiO_2, with water as the base fluid were considered.

The subject of the work is deduced in the accompanying way.

i) The momentum boundary layer thickness enhances while velocity profile reduces for larger values of magnetic parameter β.

ii) It is delineated that the induced magnetic profile diminishes, while the thermal boundary layer thickness and temperature distribution enhances with an increment in β.

iii) The induced magnetic profile decreases with expanding the values of *M*.

iv) The impact of volume friction has been watched that expanding the ϕ, the momentum boundary layer and induced boundary layer thickness enhances, while the thermal

boundary layer reduces gradually.

v) The axial velocity and induced magnetic profile are higher for Cu/water compared with the other.

vi) Velocity profile increase, while induced magnetic field and temperature profile decrease, with an increase in β_0.

vii) For various value of wedge parameter λ the axial velocity and induced magnetic field increases while temperature field decrease.

Bibliography

1) S.K. Das, S.U.S Choi, W. Yu, and T. Pradeep. *Nanofluids: science and technology*. John Wiley & Sons, 2007.
2) X.Q. Wang, and A.S. Mujumdar, "Heat transfer characteristics of nanofluids: a review." *International journal of thermal sciences* 46, no. 1 (2007): 1-19.
3) H. Chen, and Y. Ding. "Heat transfer and rheological behavior of nanofluids–a review." In *Advances in transport phenomena*, pp. 135-177. Springer Berlin Heidelberg, 2009.
4) S.U.S. Choi, Enhancing thermal conductivity of fluids with nanoparticles, in: The Proceedings of the 1995 ASME Int. Mechanical Engineering Congress and Exposition, ASME, San Francisco, USA, 1995, pp. 99e105. FED 231/MD 66.
5) K. Khanafer, K. Vafai, and M. Lightstone. "Buoyancy-driven heat transfer enhancement in a two-dimensional enclosure utilizing nanofluids." *International Journal of Heat and Mass Transfer* 46, no. 19 (2003): 3639-3653.
6) R.U. Haq, S. Nadeem, Z. H. Khan, and N. F. M. Noor. "MHD squeezed flow of water functionalized metallic nanoparticles over a sensor surface." *Physica E: Low-dimensional Systems and Nanostructures* 73 (2015): 45-53.
7) Y. Lin, L. Zheng, X. Zhang, L. Ma, and G. Chen. "MHD pseudo-plastic nanofluid unsteady flow and heat transfer in a finite thin film over stretching surface with internal heat generation." *International Journal of Heat and Mass Transfer* 84 (2015): 903-911.
8) S. Nadeem, and N. Muhammad. "Impact of stratification and Cattaneo-Christov heat flux in the flow saturated with porous medium." *Journal of Molecular Liquids* 224 (2016): 423-430.
9) S. Nadeem, and C. Lee. "Boundary layer flow of nanofluid over an exponentially stretching

surface." *Nanoscale Research Letters* 7, no. 1 (2012): 1-6.

10) O.A. Bég, A.Y. Bakier, V.R. Prasad, J. Zueco, and S. K. Ghosh. "Nonsimilar, laminar, steady, electrically-conducting forced convection liquid metal boundary layer flow with induced magnetic field effects." *International Journal of Thermal Sciences* 48, no. 8 (2009): 1596-1606.
11) B. Singh, and P. K. Agarwal. "Numerical solution of a singular integral equation appearing in magnetohydrodynamics." *Zeitschrift für angewandte Mathematik und Physik ZAMP* 35, no. 6 (1984): 760-770.
12) M. Kumari, H.S. Takhar, and G. Nath. "MHD flow and heat transfer over a stretching surface with prescribed wall temperature or heat flux." *Wärme-und Stoffübertragung* 25, no. 6 (1990): 331-336.
13) H.S. Takhar, M. Kumari, and G. Nath. "Unsteady free convection flow under the influence of a magnetic field." *Archive of Applied Mechanics* 63, no. 4-5 (1993): 313-321.
14) F.M. Ali, R. Nazar, N. M. Arifin, and I. Pop. "MHD stagnation-point flow and heat transfer towards stretching sheet with induced magnetic field." *Applied Mathematics and Mechanics* 32, no. 4 (2011): 409-418.
15) S. Nadeem, and S. Akram. "Peristaltic flow of a couple stress fluids under the effect of induced magnetic field in an asymmetric channel." *Archive of Applied Mechanics* 81, no. 1 (2011): 97-109.
16) K.S Mekheimer. "Effect of the induced magnetic field on peristaltic flow of a couple stress fluid." *Physics Letters A* 372, no. 23 (2008): 4271-4278.
17) B.K. Dutta, "Heat transfer from a stretching sheet in hydromagnetic flow." *Wärme-und Stoffübertragung* 23, no. 1 (1988): 35-37.

18) Andersson, Visiting Prof HI. "MHD flow of a viscoelastic fluid past a stretching surface." *Acta Mechanica* 95, no. 1-4 (1992): 227-230.

19) I. Pop and T.Y. Na. "A note on MHD flow over a stretching permeable surface." *Mechanics Research Communications* 25, no. 3 (1998): 263-269.

20) S.P.A. Devi, and M. Thiyagarajan. "Steady nonlinear hydromagnetic flow and heat transfer over a stretching surface of variable temperature." *Heat and Mass Transfer* 42, no. 8 (2006): 671-677.

21) F.M. Ali, R. Nazar, N.M. Arifin, and I. Pop. "MHD boundary layer flow and heat transfer over a stretching sheet with induced magnetic field." *Heat and mass transfer* 47, no. 2 (2011): 155-162.

22) F.M. Ali, R. Nazar, N. M. Arifin, and I. Pop. "MHD stagnation-point flow and heat transfer towards stretching sheet with induced magnetic field." *Applied Mathematics and Mechanics* 32, no. 4 (2011): 409-418.

23) J.P. Abraham, and E.M. Sparrow. "Friction drags resulting from the simultaneous imposed motions of a freestream and its bounding surface." *International Journal of Heat and Fluid Flow* 26, no. 2 (2005): 289-295.

24) E.M. Sparrow, and J.P. Abraham. "Universal solutions for the streamwise variation of the temperature of a moving sheet in the presence of a moving fluid." *International Journal of Heat and Mass Transfer* 48, no. 15 (2005): 3047-3056.

25) B.C. Sakiadis, "Boundary-layer behavior on continuous solid surfaces: I. Boundary-layer equations for two-dimensional and axisymmetric flow." *AIChE Journal* 7, no. 1 (1961): 26-28.

26) N.A. Yacob, A. Ishak, and I. Pop. "Falkner–Skan problem for a static or moving wedge in

nanofluids." *International Journal of Thermal Sciences* 50, no. 2 (2011): 133-139.

27) A. Asaithambi, "A finite-difference method for the Falkner-Skan equation." *Applied Mathematics and Computation* 92, no. 2 (1998): 135-141.

28) M.B. Zaturska, and W. H. H. Banks. "A new solution branch of the Falkner-Skan equation." *Acta Mechanica* 152, no. 1-4 (2001): 197-201.

29) H.T. Yang, and L. C. Chien. "Analytic Solutions of the Falkner-Skan Equation when β=-1 and γ=0." *SIAM Journal on Applied Mathematics* 29, no. 3 (1975): 558-569.

30) T. Fang, and J. Zhang. "An exact analytical solution of the Falkner-Skan equation with mass transfer and wall stretching." *International Journal of Non-Linear Mechanics* 43, no. 9 (2008): 1000-1006.

31) A.P.D.TWatanabe. "Thermal boundary layers over a wedge with uniform suction or injection in forced flow." *Acta Mechanica* 83, no. 3-4 (1990): 119-126.

32) K.A. Yih. "Uniform suction/blowing effect on forced convection about a wedge: uniform heat flux." *Acta Mechanica* 128, no. 3-4 (1998): 173-181.

33) F.M. White, Viscous Fluid Flow, 3rd ed. McGraw-Hill, New York, 2006.

34) H. F. Oztop, and E. Abu-Nada. "Numerical study of natural convection in partially heated rectangular enclosures filled with nanofluids." *International journal of heat and fluid flow* 29, no. 5 (2008): 1326-1336.